

Electrochemical remediation of metal-bearing wastewaters Part II: Corrosion-based inhibition of copper removal by iron (III)

T. L. HATFIELD, D. T. PIERCE*

Department of Chemistry, University of North Dakota, Grand Forks, ND 58202, USA

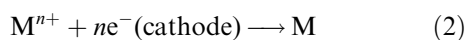
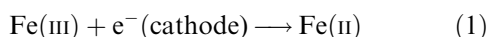
Received 20 September 1996; revised 7 March 1997

A hitherto undocumented inhibition to electrodeposition of Cu(II) from dilute (<200 mg L⁻¹) wastewaters was traced to the presence of Fe(III) at concentrations comparable to those of copper ion. This inhibition was found to differ from heterogeneous side-reduction of Fe(III) that is well known to decrease faradaic efficiency for copper removal. Based on bench-scale electrolysis as well as cyclic voltammetry studies, an inhibition mechanism was qualitatively identified that involved copper corrosion by Fe(III). This corrosion process was found to be strongly favoured by sluggish heterogeneous reduction of Fe(III) at carbon electrode materials. One procedure shown to substantially improve copper removal from solutions demonstrating corrosion inhibition was alkali precipitation of iron. Real mine drainage wastewater that was pretreated in this manner was consistently depleted of copper by flow-through electrolysis to levels below 50 µg L⁻¹.

Keywords: *copper removal, wastewater, iron (III)*

1. Introduction

A great number of methods have been reviewed [1–4], tested [5–12] and even commercialized [2, 13] for the removal of environmentally harmful metal ions from wastewater by electrodeposition onto porous cathodes. Our own work has focused on the removal of copper from relatively dilute wastestreams associated with mine drainage and run-off [12]. Although our system and many others [5–11] have been successful in treating refined or simulated wastewaters containing only one metal component, a sizable body of research has demonstrated that electrodeposition is inhibited for more complex solutions which carry significant quantities of iron [14–24]. Because it is well known that Fe(III) is reduced to Fe(II) at voltages appropriate for the electrodeposition of most target metals (M = Cu, Cd and Ni), the source of this inhibition has generally been ascribed to the side-reaction of ferric ion (Equation 1) that competes for current with the metal deposition process (Equation 2):

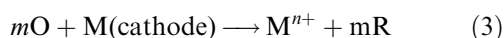


Inhibition by this side-reaction has typically been diagnosed by measurements of current efficiency for the deposition reaction at different Fe(III) concentrations [15, 20].

Despite ample documentation of an iron inhibition mechanism described by Equations 1 and 2, the work

described in this paper demonstrates that this model may be incorrect under certain conditions commonly encountered during remediation of environmental solutions. The first condition pertains to dilute solutions of the target metal ion (<200 mg L⁻¹) and the second corresponds to sluggish heterogeneous reduction of Fe(III) at carbon electrode materials.

Sioda has investigated the first condition and described the inhibition characteristics associated with electrodeposition from dilute solutions in the low ppm (mg L⁻¹) to ppb (µg L⁻¹) range [25–28]. Central tenants of this work were that metal deposits can be partially redissolved and that metal ions can be returned to solution despite the cathode being poised at negative potentials [25]. It was shown by model calculations that when the concentration of an electrodeposited metal ion is low, competing formation and dissolution rates of the deposit can produce a steady-state that holds the metal ion concentration constant and thereby inhibits further metal removal [27]. Experiments established that the dissolution reaction was a corrosion process (Equation 3) initiated by a chemical oxidant (O) present in solution [26]:



Although dissolved oxygen was recognized as the most likely oxidant because of its ubiquity, it was also suggested that other oxidizing agents such as chlorine and nitric acid could participate [28]. Interestingly, Fe(III) was not listed among these oxidants and its participation in a corrosion inhibition process has not been documented in any electrodeposition study to date. This is unusual since Fe(III) would appear to be

* Author to whom correspondence should be addressed.

an excellent candidate to perturb electrodeposition by Equation 3 ($O = \text{Fe(III)}$, $R = \text{Fe(II)}$) since its corrosion of wide variety of metals ($M = \text{Ag, Cu and Hg}$) in assorted media (Cl^- and SO_4^{2-}) is known to be quite facile [29–35].

The present work was designed to assess whether iron-based corrosion actively inhibits electrodeposition of copper from relatively dilute solutions. Because ferric ion is prevalent in many environmental wastewaters, corrective measures to improve copper removal were tested with the iron-rich wastewater associated with mine drainage.

2. Experimental details

2.1. Materials

Electrolyte standards were prepared with Na_2SO_4 and concentrated H_2SO_4 in 18 M Ω cm Milli-Q reagent water (Millipore Co.). Copper(II) sulfate as well as iron(II) and iron(III) sulfates were dissolved in stock electrolyte to produce standard solutions ($\pm 0.1\%$). Oxygen was removed from solutions by sparging with either compressed argon or nitrogen that was first passed through an oxygen scrubber column.

Real wastewater samples from the 2 m and 60 m levels of the defunct Berkeley mine drainage pit in Butte, Montana (USA) were collected in 20 L oxygen and light-impermeable containers. The containers were transported within 48 h to laboratories at the University of North Dakota and stored at 4 °C until treated or analysed. Elemental and ion analyses of the water samples were carried out by EPA-certified laboratories of the Energy and Environmental Research Center at the University of North Dakota. Some additional handling precautions were taken with samples of the 60 m waters. Prior to electrolytic treatment, 60 m water samples were transferred under argon from their storage containers into an argon-purged reservoir for the flow-through electrolysis cell. Care was also taken to protect the 60 m samples from light during all handling and treatment procedures since these solutions appeared to change colour rapidly even under normal room light. All samples were analysed and treated within 30 d of collection.

2.2. Instrumentation and procedures

Copper and iron concentrations in all electrolysed solutions were screen by flame atomic absorption spectroscopy (FAAS) with the spectrometer (Perkin–Elmer model 2280) aligned to the 324.8 nm hollow-cathode emission of copper or 248.3 nm emission of iron. Copper concentrations below the 10 mg L⁻¹ detection limit of the FAAS instrument were measured by anodic stripping voltammetry (ASV) at a renewable hanging mercury drop electrode (EG&G model 303). FAAS and ASV analysis were accurate to $\pm 1\%$.

Flow-reactor studies were carried out with a bench-scale, flow-through cell. Auxiliary apparatus

and operating procedures for this cell have been described in detail [12].

Batch-reactor studies were performed on 50 mL solution aliquots contained in an airtight, frit-separated, two-compartment glass cell. Controlled-potential coulometry (CPC), cyclic voltammetry (CV), and chronoamperometry (CA) experiments were controlled with an EG&G model 273 potentiostat. A platinum mesh cylinder was submerged in the counter-electrode compartment and a fritted saturated calomel reference electrode (SCE) was positioned within the working electrode compartment. The working electrode used for CPC was a partially-submerged 0.5 g bundle of the same carbon felt used in the flow-through cell (Amoco THORNE Mat VMA). Working electrodes used for CV and CA were discs of glassy-carbon (3.2 mm dia.) or platinum (2.4 mm dia.) imbedded in Kel-F (Bioanalytical Systems). The working-electrode headspace as well as its solution was purged with either purified nitrogen or compressed air. Solution concentrations of Cu(II) were monitored during CPC by extracting 50.0 μL aliquots which were diluted to 5.00 mL and analysed by FAAS or ASV. During CPC, the working-electrode solution was stirred at a constant rate with a magnetic stir bar.

All electrode potentials were referenced to the silver/silver chloride couple (3.5 M KCl) unless otherwise noted.

3. Results and discussion

3.1. Batch-reactor studies of iron corrosion effects

The results of batch CPC of copper electrodeposition in the presence or absence of Fe(II), Fe(III) and dissolved oxygen are summarized in Table 1. Logarithmic decays of electrolytic current with time and near 100% coulometric efficiencies demonstrated that the presence of Fe(II) or dissolved oxygen did not inhibit the electrodeposition of copper. Although the negligible influence of dissolved oxygen at first appeared to contradict findings of Ciszewski *et al.* for corrosion inhibition of copper electrodeposition (Equations 2 and 3, $O = \text{O}_2$) [26], it was noted that the concentration of Cu(II) during batch testing was always above 0.5 mg L⁻¹. This level was significantly higher than concentration levels implicated by Ciszewski *et al.*, who only observed inhibition by dissolved oxygen when Cu(II) concentrations were below 200 $\mu\text{g L}^{-1}$.

The presence of Fe(III) in solution clearly affected the electrodeposition of copper. For two concentrations of iron (212 mg L⁻¹ and 118 mg L⁻¹), the current efficiency for copper deposition was decreased by 40% and 30%, respectively. These decreases reflected the excess charge required to quantitatively electrolyse Fe(III) to Fe(II) and, without further diagnosis, appeared to confirm the simple inhibition mechanism given by Equations 1 and 2. However, closer examination of other electrolysis data in Figs 1 and 2 indicated three clear discrepancies with this model.

Table 1. Results from batch-reactor coulometry* of copper electrodeposition

Initial system [†]	Φ'_{Cu}	$[Cu^{2+}]_f/mg\ L^{-1}$	$[Fe^{3+}]_f/mg\ L^{-1}$	ΔpH
Cu(II)	0.94	0.681		0.0
Cu(II)/O ₂ [‡]	0.96	0.615		0.0
Cu(II)/Fe(II)	1.04	0.426	0.00	0.0
Cu(II)/Fe(III)	0.64	0.036	212	+0.5
Cu(II)/Fe(III)	0.72	0.258	118	+0.3
Cu(II)/Fe(III) [§]	0.82	0.055	(0.5)**	0.0

* Column headings have the following definitions: current efficiency for copper reduction (Φ'_{Cu}) was calculated as ratio of charge predicted for exhaustive plating of copper to the total charge passed during electrolysis; species concentrations ($[]_{i,f}$) were determined before (i) or after (f) electrolysis; change in solution pH (ΔpH) was determined from pH measurements made before and after electrolysis.

[†] Unless otherwise noted, initial solutions were adjusted to pH 2.8, thoroughly sparged with nitrogen, and contained 0.1 M Na₂SO₄, copper at 151 mg L⁻¹, iron at 100–200 mg L⁻¹.

[‡] Initial solution contained oxygen at its air saturated limit of 8–9 mg L⁻¹ (20 °C).

[§] Initial solution was adjusted to pH 4.2 and precipitated iron hydroxides were removed by filtration before electrolysis.

** Concentration was determined after filtration but before electrolysis.

First, with Fe(III) and Cu(II) present together the electrolysis current (Fig. 1(b)) did not show a simple exponential decrease that would have characterized a diffusion-controlled reduction of both components. Instead, an anomalous plateau was observed early in the electrolysis when the current was still about 80% of its initial value. A second deviation was evident from the constant concentration of Cu(II) measured in the same 20–100 s period of the electrolysis (Fig. 2(b)). If Cu(II) had been reduced without any influence from a competing dissolution reaction, its concentration would have decreased exponentially as in Fig. 2(a). Thirdly, it was noted in repeated experiments that when an electrolysis was halted within the anomalous 20–100 s period and then resumed, the current had increased to its initial value.

All three effects were qualitatively diagnostic of a heterogeneous reaction that returned Cu(II) to solution during the anomalous period of 20–100 s [36]. Because no other oxidant was present during these experiments, it was evident that this heterogeneous process was an Fe(III) corrosion reaction similar to that proposed by Sioda *et al.* [25] (Equation 3: M = Cu, n = 2, m = 2, O = Fe(III), R = Fe(II)).

However, uncertainties associated with mass transfer and large concentration perturbations of the CPC technique precluded further diagnosis by this method.

CV and CA at microdisc electrodes showed more clearly why the corrosion process might have predominated over heterogeneous side-reaction of Fe(III) to inhibit copper deposition. Figure 3 compares CV traces recorded for the Fe(III/II) couple in sulfate media with glassy carbon and platinum working electrodes.

Peak separations of the Fe(III/II) couple at the carbon electrode were considerably greater than the Nernstian limit of 60 mV and were diagnostic of slow heterogeneous electron transfer [37]. It is well known that the Fe(III/II) couple is kinetically hindered at glassy carbon, graphite, and other carbonaceous materials [38]. Because the Fe(III/II) reaction was particularly slow at the carbon felt used for CPC, necessitating extremely large overpotentials for electrolysis (e.g., -0.8 V vs Ag/AgCl in Figs 1 and 2), it was evident that this effect might have kinetically favoured copper corrosion (Equation 3) over the thermodynamically preferred heterogeneous reduction (Equation 1). Specifically, if slow heterogeneous

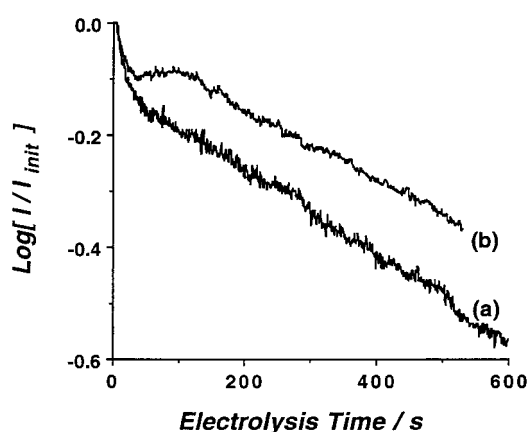


Fig. 1. Log-current against time curves for batch electrolyses of deoxygenated solutions containing (a) 236 mg L⁻¹ Cu(II) in 0.1 M Na₂SO₄ (pH 2.60) or (b) 130 mg L⁻¹ Cu(II) and 213 mg L⁻¹ Fe(III) 0.1 M Na₂SO₄ (pH 2.60). Electrolysis potential was -0.8 V vs Ag/AgCl.

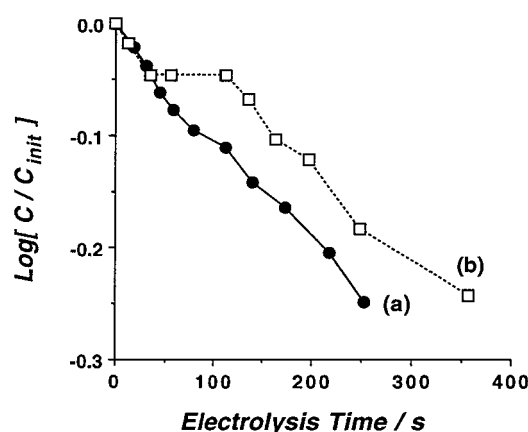


Fig. 2. Log-copper concentration against time curves for batch electrolyses of deoxygenated solutions containing (a) 236 mg L⁻¹ Cu(II) in 0.1 M Na₂SO₄ (pH 2.60) or (b) 130 mg L⁻¹ Cu(II) and 213 mg L⁻¹ Fe(III) 0.1 M Na₂SO₄ (pH 2.60). Electrolysis potential was -0.8 V vs Ag/AgCl.

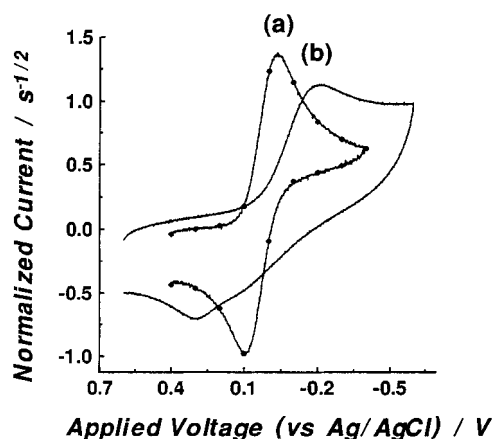


Fig. 3. Cyclic voltammograms of the Fe(III/II) couple recorded at 100 mV s^{-1} with a (a) platinum disc and (b) glassy-carbon disc electrode. Solution conditions of 212 mg L^{-1} Fe(III) in $0.1 \text{ M Na}_2\text{SO}_4$ (pH 2.60) were identical for each trace. Currents were normalized with the Cottrell constant (i.e., $nFAC^*(D/\pi)^{1/2}$) measured by CA at the negative CV potential limit.

reduction permitted large surface concentrations of Fe(III) at potentials appropriate for copper plating, the rate of corrosion by Equation 3 might have been increased to compete with the rate of metal deposition. Such competition would account for the steady-state of copper concentration within the 20–100 s period of Fig. 2(b).

Corrosion inhibition of copper electrodeposition was effectively eliminated by solution treatments that removed Fe(III) before electrolysis. For the present bench-scale work, Fe(III) was removed by rendering solutions basic with NaOH and thereby precipitating Fe(III) as the hydroxide. Because Cu(II) hydroxide is much more soluble than Fe(III) hydroxide, careful pH control was not necessary and addition of base to about pH 4–5 was sufficient to selectively precipitate Fe(III)*. FAAS analysis of the solution after alkali pretreatment confirmed that less than 10% of Cu(II) was lost by coprecipitation of Cu(II) ions with Fe(III) hydroxide. Following precipitation and decantation, electrolysis of the supernatant solution proceeded with current decreasing rapidly and exponentially towards zero and copper concentration decreasing by more than 99.9%.

3.2. Flow-reactor studies of iron corrosion effects

Because of the ability to monitor solution concentrations during electrolysis, batch-reactor experiments were generally more diagnostic of corrosion inhibition. However, the greater utility of flow-reactors for treating high volume, environmental solutions indicated that some testing with this design would be beneficial. A previously designed flow-

through reactor [12] was used to assess Fe(III) corrosion effects on copper removal. Figures 4 and 5 show ohmic-corrected polarization curves obtained with this reactor for solutions that contained mixtures of Cu(II) with Fe(II) or with Fe(III).

The steady-state currents recorded for the Cu(II)/Fe(II) solution (Fig. 4(a)) showed a distinct plateau from about -0.5 to -0.75 V vs Ag/AgCl. This feature indicated mass-transfer limited deposition of copper throughout the porous cathode since, at these potentials, the concentration of copper in the cathode effluent was greatly diminished (Fig. 4(b)). Also, the limiting current was approximately equal to 70 mA , the value predicted by Faraday's law for complete electrolytic removal of copper ion with 100% current efficiency. At potentials below -0.75 V , the steady-state current showed a sharp rise that correlated with increased pH of the catholyte effluent and hydrogen bubble nucleation on copper deposits at the cathode entrance. These characteristics indicated the onset of proton reduction.

Because polarization characteristics exhibited by solutions containing Fe(II) were very similar to features observed for solutions containing only Cu(II) ions [12], Fe(II) clearly did not inhibit copper electrodeposition during flow-through electrolysis. However, polarization behaviour of the Cu(II)/Fe(III) solution differed significantly from solutions containing Cu(II)/Fe(II) or copper ion alone. Figure 5 shows that no copper was removed over the potential range of -0.5 to -0.75 V although a current plateau, indicative of a mass-transfer limited process, was evident.

Although this limiting current was greater than predicted for total consumption of copper (70 mA), it was also significantly less than expected for simultaneous and complete reduction of Cu(II) and Fe(III) (123 mA). Oddly, the increase in steady-state current at potentials negative of -0.75 V was not caused by proton reduction because the pH of cathode effluent

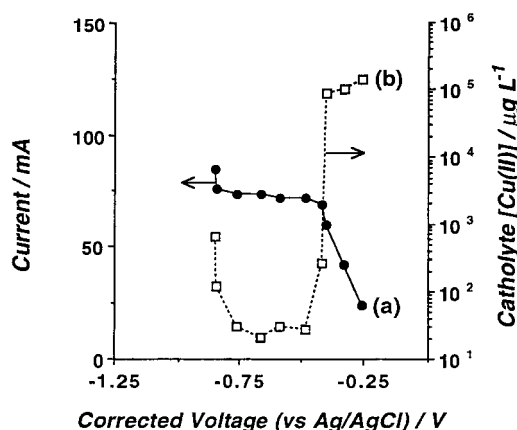


Fig. 4. Ohmic-corrected (10Ω) polarization curves showing (a) steady-state current (in mA) and (b) copper ion concentration in the catholyte effluent (in $\mu\text{g L}^{-1}$). Cathode length, mass and flow rate were 1.9 cm , 1.8 g and 0.15 mL s^{-1} , respectively. Entering solution contained 150 mg L^{-1} Cu(II), 225 mg L^{-1} Fe(II) and $0.01 \text{ M Na}_2\text{SO}_4$ (pH 2.60).

* Concentrations of Cu(II) and Fe(III) that initiate hydroxide precipitation are calculated from the solubility product expressions for $\text{Cu}(\text{OH})_2$ ($K_{\text{sp}} = 4.8 \times 10^{-20}$) and $\text{Fe}(\text{OH})_3$ ($K_{\text{sp}} = 2 \times 10^{-39}$). For a solution pH range of 4–5, the limiting concentration of Cu(II) is about 5 to 0.05 M while the limiting concentration for Fe(III) is about 10^{-9} to 10^{-12} M .

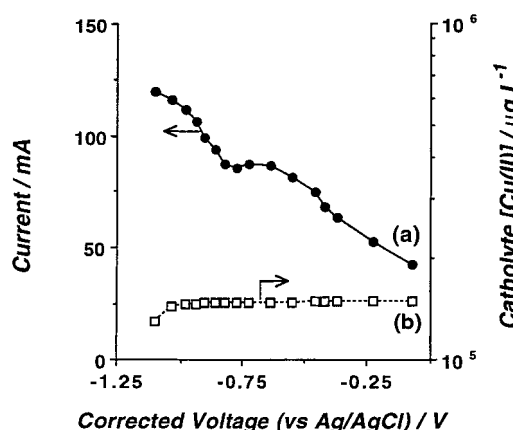


Fig. 5. Ohmic-corrected ($10\ \Omega$) polarization curves showing (a) steady-state current (in mA) and (b) copper ion concentration in the catholyte effluent (in $\mu\text{g L}^{-1}$). Cathode length, mass and flow rate were 1.9 cm, 1.8 g and $0.16\ \text{mL s}^{-1}$, respectively. Entering solution contained $150\ \text{mg L}^{-1}\ \text{Cu}^{2+}$, $212\ \text{mg L}^{-1}\ \text{Fe}^{3+}$ and $0.10\ \text{M}\ \text{Na}_2\text{SO}_4$ (pH 2.60).

was not affected and no hydrogen evolution was observed. At potentials less than $-1.0\ \text{V}$, the current again showed signs of reaching a limit that was nearly equal to the value calculated for quantitative reduction of both Cu(II) and Fe(III) . Only as this second limiting current was approached did the copper concentration in the cathode effluent decrease.

Information provided by Fig. 5 clearly contradicts the simple mechanism of deposition inhibition specified by Equation 1 and 2. However, it does support a corrosion-based process (Equations 2 and 3). At about $-0.7\ \text{V}$, where mass-transfer controlled copper deposition occurred with solutions of Cu(II) or Cu(II)/Fe(II) , the Cu(II)/Fe(III) solution showed no evidence of Cu(II) loss from solution or of copper metal adherence to cathode fibres. This could not have occurred unless a reaction was active that redissolved copper metal as it deposited on the cathode (i.e., Equation 3). The fact that a limiting current was observed at these potentials also suggested that the combined deposition and dissolution process was sufficiently rapid to be controlled by mass-transfer. This finding was consistent with corrosion studies of the Fe(III)/Cu system in acidic sulfate media [35].

Other unusual features of Fig. 5 were consistent with sluggish heterogeneous reductions of proton and Fe(III) at the carbon felt cathode. It is well known that both processes are slow and require high overpotentials at carbon electrode materials [38]. Because no copper metal was deposited from the Cu(II)/Fe(III) solutions, no substrate was available to enhance the rate of either reduction. The consequence for proton was that no pH change or hydrogen evolution occurred within the potential window from -0.70 to $-1.0\ \text{V}$. The consequence for Fe(III) was that reduction to Fe(II) at the electrode (Equation 1) was only rapid at potentials negative of the copper deposition process. Specifically, only at potentials approaching $-1.0\ \text{V}$ did the reaction become controlled by mass-transfer and yield a limiting current that corresponded to exhaustive consumption of both Fe(III)

and Cu(II) ions. This sluggish heterogeneous reduction probably enhanced copper corrosion at potentials lower than $-1.0\ \text{V}$ because a greater number of Fe(III) ions were available in solution to react with deposited metal (Equation 3). Only at potentials negative of $-1.0\ \text{V}$ did Cu(II) concentration decrease in the catholyte and copper begin to deposit.

3.3. Copper removal from real mine drainage waters

To demonstrate the effects of corrosion inhibition for real wastewaters and to test the efficacy of corrective procedures, mine drainage with high iron content was electrolysed to remove copper. Studies of real waters were performed by flow-through electrolysis.

3.3.1. Predicted interferences. Table 2 shows the results from a detailed analysis of drainage waters collected from the 2 m and 60 m levels of the closed Berkeley copper mine pit at Butte, Montana (USA). Comparison of this list with a list of standard deposition potentials suggested that copper could be selectively separated from most of the metal constituents present in both the 2 m or 60 m waters. Mercury was the only species present that was thermodynamically favoured to deposit with copper. However, because mercury was only present at concentrations about 2000 times lower than copper, its codeposition was not expected to be significant.

The data in Table 2 were also useful for predicting susceptibility to an iron-based corrosion process. Water from 2 m was initially chosen for treatment

Table 2. Elemental and ionic compositions of water samples collected from 2 m and 60 m depths of the Berkeley mine drainage pit at Butte, Montana (USA)

Parameter	2 m level	60 m level
<i>Major elements*</i> (mg L^{-1})		
Al	120	130
Ca	440	450
Cu	180	150
Fe	320	1100
Fe(II)^\ddagger	< 1 [†]	1000
Fe(III)^\ddagger	140	120
Mg	440	420
Mn	190	210
Na	74	80
Zn	510	620
<i>Detectable minor elements*</i> (mg L^{-1})		
Cd	2.0	1.9
Co	1.2	0.9
Hg	0.100	d
Ni	0.98	0.9
<i>Anions</i> [‡] (mg L^{-1})		
Cl^-	16	20
SO_4^{2-}	6900	8300
Conductivity ($10^3 \times \Omega^{-1}\ \text{cm}$)	4.21	4.43
pH	2.87	3.00

* Analysis performed by inductively coupled argon plasma unless otherwise noted.

[†] Concentration below detection limit of instrument.

[‡] Analysis performed by ion chromatography.

because of sampling convenience. However, complete aeration of this matrix ensured that iron was present exclusively in its 3+ state. To test a potentially less corrosive matrix, water was collected at a lower depth (60 m) that was well below the summer thermocline. At this level the water was free of dissolved oxygen and was expected to contain a higher proportion of Fe(II). Although the 60 m matrix did contain nearly 90% Fe(II), the total amount of solubilized iron was greater at this depth and the Fe(III) concentration was nearly the same as the 2 m matrix. For this reason, it was anticipated that copper recovery from both solutions would be inhibited.

3.3.2. Results for raw wastewaters. Figure 6 shows ohmic-corrected polarization curves acquired during the flow-through electrolysis of raw 2 m water. Although no current plateau was observed before reaching proton reduction at extreme negative potentials, a catholyte flow rate of 0.14 mL s^{-1} did produce a moderate decrease in copper concentration to 39 mg L^{-1} at an ohmic corrected voltage of -0.9 V vs Ag/AgCl. Slowing the flow rate to 0.1 mL s^{-1} decreased the copper content in the catholyte effluent further to 1.0 mg L^{-1} . However, use of flow rates less than 0.1 mL s^{-1} caused Cu(II) concentration to increase. This probably resulted because of mixing between the unseparated cathode and anode solutions as their flow rates became comparable [12].

Electrolysis of 60 m water at a catholyte flow rate of 0.12 mL s^{-1} produced a moderate improvement in copper removal compared to the 2 m water (15 mg L^{-1} vs 39 mg L^{-1} in effluent). This improvement may have resulted from the slightly lower matrix concentration of Fe(III). However, severe air and light-sensitivity of these subthermocline solutions made routine treatment impracticable for improving copper removal.

3.3.3. Results for alkali pretreated wastewater. Pre-treatment to precipitate Fe(III) closely followed the

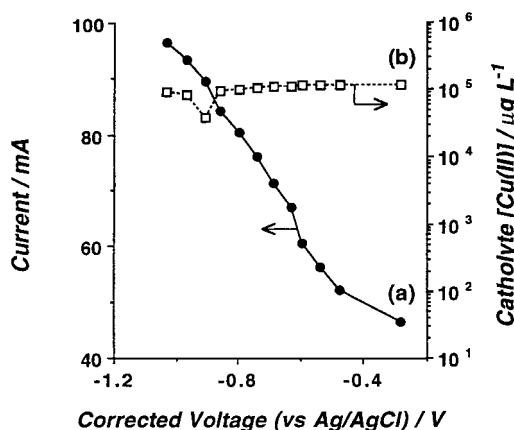


Fig. 6. Ohmic corrected (10Ω) polarization curves recorded during the flow-through electrolysis of raw 2 m drainage water collected from the Berkeley pit site at Butte, Montana (USA). Curves show (a) steady-state current (in mA) and (b) copper ion concentration in the catholyte effluent (in $\mu\text{g L}^{-1}$). Cathode length, mass and flow rate were 1.9 cm , 1.7 g and 0.14 mL s^{-1} , respectively.

procedure worked out in batch-reactor studies. Specifically, 2 m water was adjusted to a pH of 4–5 by addition of NaOH ($\sim 0.7 \text{ g L}^{-1}$ of 2 m water). The adjusted solution was allowed to stand for 24 h after which the precipitated Fe(III) oxide and hydroxides were removed by decantation. FAAS analysis of the supernate before electrochemical treatment confirmed less than 10% loss of the copper ion by co-precipitation. Figure 7 shows polarization curves obtained for a solution of alkali-treated 2 m water.

Unlike the polarization curves of unadjusted water samples (e.g., Fig. 5), the pH adjusted samples demonstrated curves with a definite limiting current that indicated a mass-transfer controlled reaction occurring throughout the cathode. Because the plateau was only observed at potentials where significant copper deposition occurred (dashed curve), the cathode reaction was certainly one involving copper deposition. The good correlation between the measured plateau and the limiting current predicted by Faraday's law for quantitative copper removal ($\sim 60 \text{ mA}$) indicated nearly 100% current efficiency for the copper deposition reaction. Also, the lowest concentration of copper ion in the treated catholyte ($27 \mu\text{g L}^{-1}$) matched the minimum concentration predicted for the flow-through cell [12].

Although alkali pretreatment appeared to be an effective bench-scale procedure for correcting corrosion inhibition associated with iron-rich wastewaters, it was clear, as we have previously noted [12], that metal hydroxide sludge generation and stabilization pose severe drawbacks to treatment at a commercial scale. Our attempts to remediate potentially less corrosive, subthermocline solutions were unsuccessful because of air and light sensitivity of this matrix. More viable solutions to the problem will necessitate new cell designs to decrease the inlet concentration of Fe(III) (e.g., pre-electrolysis, periodic current reversal, or homogeneous reduction to Fe(II)) [39], enhance the kinetics of heterogeneous Fe(III) reduction (e.g., noncarbon cathode material), or decrease the corro-

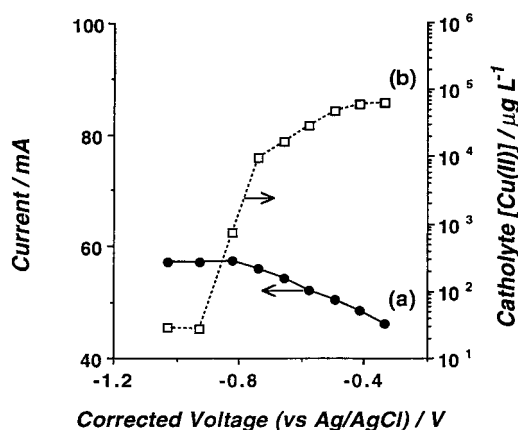


Fig. 7. Ohmic corrected (10Ω) polarization curves recorded during the flow-through electrolysis of pH adjusted 2 m drainage water. Curves show (a) steady-state current (in mA) and (b) copper ion concentration in the catholyte effluent (in $\mu\text{g L}^{-1}$). Cathode length, mass and flow rate were 4.4 cm , 2.3 g and 0.12 mL s^{-1} , respectively.

siveness of Fe(III) prior to electrowinning (e.g., complexation).

4. Conclusions

Solutions containing high ppm concentrations of Fe(III) were found to strongly inhibit the electrochemical removal of copper ions from real and simulated mine drainage waters. Controlled tests conducted at qualitative levels showed that the process involved copper corrosion by Fe(III). It was found that this corrosion process was kinetically favoured by slow heterogeneous reduction of Fe(III) at carbon electrodes. Although impractical at a commercial scale, the inhibition process was virtually eliminated at bench scales by alkali precipitation of Fe(III) prior to electrochemical treatment.

Acknowledgements

We thank D. Hassett, J. Thompson, F. Beaver, and J. Harju of the UND Energy and Environmental Research Center for permission to quote unpublished results from their sampling and detailed analysis drainage waters from the Berkeley Pit Site. We also acknowledge the donors of the Petroleum Research Fund, administered by the American Chemical Society, for partial support of this as well as the generous support the North Dakota EPSCoR program and the US Bureau of Mines under Allotment Grant G11344238.

References

- [1] L. E. Vaaler, *AIChE Symp. Ser.* **77** (1981) 171.
- [2] J. L. Weininger *ibid.* **79** (1983) 179.
- [3] R. E. Sioda and K. B. Keating, *Electroanal. Chem.* **12** (1982) 1.
- [4] J. Farka and G. D. Mitchell, *AIChE Symp. Ser.* **81** (1985) 57.
- [5] R. S. Wenger and D. N. Bennion, *J. Appl. Electrochem.* **6** (1976) 385.
- [6] S. C. Das, *J. Electrochem. Soc. India* **27** (1978) 235.
- [7] R. E. Sioda and H. Piotrowska, *Electrochim. Acta* **25** (1980) 331.
- [8] J. Legrand, J. M. Marracino and F. Coeuret, *J. Appl. Electrochem.* **16** (1986) 365.
- [9] E. Avici, *J. Appl. Electrochem.* **18** (1988) 228.
- [10] K. Hoppstock, R. P. H. Garten, P. Tschopel and G. Tolg, *Fresenius J. Anal. Chem.* **243** (1992) 778.
- [11] A. J. Chaudhury and S. M. Grimes, *J. Chem. Tech. Biotechnol.* **56** (1993) 15.
- [12] T. L. Hatfield, T. L. Kleven and D. T. Pierce, *J. Appl. Electrochem.* **26** (1996) 567.
- [13] D. Pletcher and F. C. Walsh, 'Industrial Electrochemistry', Chapman & Hall, New York (1990).
- [14] K. Scott and E. M. Paton, *Electrochim. Acta* **38** (1993) 2181.
- [15] K. Scott and E. M. Paton, *ibid.* **38** (1993) 2191.
- [16] D. Schab and H. Beyer, *Metall* **46** (1992) 1147.
- [17] S. K. Gogia and S. C. Das, *J. Appl. Electrochem.* **21** (1991) 64.
- [18] D. DeFilippo, C. Dessi and A. Rossi, *ibid.* **19** (1989) 37.
- [19] B. S. Boyanov, J. D. Donaldson and S. M. Grimes, *J. Chem. Tech. Biotech.* **41** (1988) 317.
- [20] D. W. Dew and C. V. Phillips, *Hydrometallurgy* **14** (1985) 331.
- [21] *Idem, ibid.* **14** (1985) 351.
- [22] R. M. Gould and R. C. Alkire, *J. Electrochem. Soc.* **126** (1979) 2125.
- [23] R. Alkire and A. A. Mirarefi, *ibid.* **124** (1979) 1214.
- [24] M. S. Quaraishi and T. Z. Fahidy, *Chem. Ind. (London)* (1975) 377.
- [25] R. E. Sioda, *Anal. Chim. Acta* **228** (1990) 323.
- [26] A. Ciszewski, J. R. Fish, T. Malinski and R. E. Sioda, *Anal. Chem.* **61** (1989) 856.
- [27] R. E. Sioda, *Anal. Chem.* **60** (1988) 1177.
- [28] R. E. Sioda, *Anal. Lett.* **16** (1983) 739.
- [29] M. D. Benari and G. T. Hefter, *Electrochim. Acta* **36** (1991) 479.
- [30] S. L. F. A. Da Costa and S. M. L. Agostinho, *J. Electroanal. Chem.* **296** (1990) 51.
- [31] S. L. F. A. Da Costa, and S. M. L. Agostinho, *Corrosion (Houston)* **45** (1989) 472.
- [32] S. L. F. A. Da Costa, J. C. Rubin and S. M. L. Agostinho, *J. Electroanal. Chem.* **220** (1987) 259.
- [33] S. L. F. A. Da Costa, S. M. L. Agostinho, H. C. Chagas and J. C. Rubin, *Corrosion (Houston)* **43** (1987) 149.
- [34] R. A. Couchie and I. M. Ritchie, *Aust. J. Chem.* **37** (1984) 231.
- [35] G. P. Power, W. P. Staunton and I. M. Ritchie, *Electrochim. Acta* **27** (1982) 165.
- [36] A. J. Bard and L. R. Faulkner, 'Electrochemical Methods', J. Wiley & Sons, New York (1980), pp. 476–83.
- [37] R. S. Nicholson *Anal. Chem.* **37** (1965) 1351.
- [38] J.-P. Randin, in 'Encyclopedia of Electrochemistry of the Elements', Vol. 7 (edited by A. J. Bard), Marcel Dekker, New York (1976) pp. 1–291.
- [39] R. O. Loufty and N. R. Bharuch, Electrowinning of copper in the presence of high concentrations of iron, *Canada patent 1 077 884* (20 May 1980); *United States patent 4 124 460* (7 Nov. 1978), respectively.